Journal of Materials Chemistry A

Accepted Manuscript

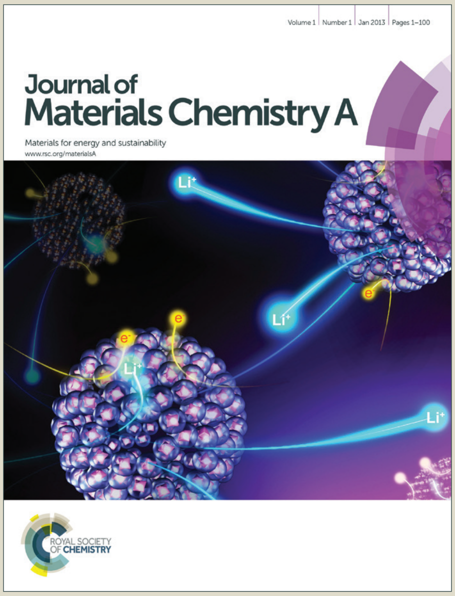

Volume 1 | Number 1 | Jan 2013 | Pages 1–100

Journal of Materials Chemistry A

Materials for energy and sustainability

www.rsc.org/materialsA

ROYAL SOCIETY OF CHEMISTRY

www.rsc.org/materialsA

Melamine-Terephthalaldehyde-Lithium Complex: A Porous Organic Network Based Single Ion Electrolyte for Lithium Ion Batteries

Rupesh Rohan,[a],‡, *Kapil Pareek,*[a]‡, *Weiwei Cai,*[a,c] *Yunfeng Zhang,* [a,c] *Guodong Xu,*[a] *Zhongxin Chen,*[a] *Zhiqiang Gao,*[a] *Zhao Dan,* [b] *Hansong Cheng**[a,c]

[a] Department of Chemistry, National University of Singapore, 3 Science Drive 3, Singapore

[b] Department of Chemical & Biomolecular Engineering, Faculty of Engineering, National University of Singapore, 4 Engineering Drive 4, Singapore.

[c] Sustainable Energy Laboratory, Faculty of Materials Science and Chemistry, China University of Geosciences, 388, Lumo Road, Wuhan 430074, P. R. China.

Abstract

Cationic transference number and ionic conductivity of an electrolyte are among the key parameters that regulate battery performance. In the present work, we introduce a novel concept of using porous organic frameworks as a single ion conducting electrolyte for lithium ion batteries. The synthesized lithium functionalized melamine-terephthalaldehyde framework (MTF-Li), a three dimensional porous organo-lithium complex, in the medium of organic solvents exhibits ionic conductivity comparable to the values of typical gel polymer electrolytes and the battery cell assembled with the membrane of the material performs at both room temperature and 80 °C. The rigid three dimensional framework, functioning as an anionic part of the electrolyte, reduces anionic transference number to minimum. As a consequence, the cationic transference number increases to 0.88, close to unity. In addition, by virtue of its synthesis procedure, the electrolyte displays excellent sustainability at high temperatures, which is important for battery safety as well as for enhancing the performance and longevity of the battery.

KEYWORDS: Electrolyte; single ion; porous; lithium ion battery; transference number.

1. Introduction

The concept of single ion conducting polymer electrolytes was proposed in 1994[1-3] to deal with the issue of concentration polarization and low cationic transference number [4-9] with conventional liquid inorganic salt electrolytes in lithium ion batteries and has been demonstrated successfully in the last decade.[10-16] These electrolytes consist of mainly anionic moieties lingered on polymeric chains, which remain immobile in electrochemical processes, and lithium ions attached to the anions via a weak electrostatic force due to anionic charge delocalization.[17-24] In a solid state, Li ions shuttle between electrodes via a hopping process, while in a gel state, ion transport is carried out through an organic solvent.[18, 25-31]

It has been found that appropriate porosity of an electrolyte membrane plays a significant role in lithium ion transport through the membrane.[32, 33] In a gel electrolyte, lithium ions solvated by organic molecules diffuse through the pores, which provide low resistance passages, facilitate ion conduction and ultimately enhance battery performance. In a previous study, we demonstrated the critical role of membrane porosity in battery operability enhancement by designing a macro/meso porous functionalized electrolyte membrane.[34] Templating, phase inversion and cross-linking are among the techniques used to generate the desired porosity.[34-37] However, it would be more practical for scalable production of porous membranes if chemical moieties with inherent porosity and appropriate functionality to transport lithium ions could be synthesized and utilized to fabricate electrolyte membranes. Porous materials including metal organic framework (MOF) and covalent organic framework (COFs) compounds have been developed for applications in Li based batteries as electrodes.[38-40] Recently, an attempt was made to design a MOF based electrolyte for Li-ion batteries.[41] Unfortunately, battery performance with the electrolyte could not be demonstrated. To the best of our knowledge, no porous material based solid electrolyte for Li-ion batteries with appreciable battery performance has been reported to date.

In this paper, we present a procedure for synthesizing a melamine-terephthalaldehyde porous complex. Upon reacting with lithium hydride, the acidic hydrogen atoms in the complex were replaced with highly mobile lithium ions. The material was subsequently blended with a PVDF-HFP binder and solution-cast onto a glass dish to form a single ion conducting electrolyte (SICE) membrane. A Li-ion battery cell was then assembled with the membrane and the device performance was subsequently demonstrated at room temperature as well as an elevated temperature. The material represents a new class of electrolyte compounds distinctively different from the previously reported sp^3 boron based or other polymer based single ion polymer electrolytes.[15, 17-20, 22, 24, 34] It exhibits a three dimensional network structure with natural porosity, which facilitates Li ion transport in the membrane.

2. Experimental

2.1. Synthesis of melamine-terephthalaldehyde-lithium complex (MTF-Li)

MTF-Li was synthesized in a two-step process, as depicted in Scheme 1. In the first step, we followed the procedure described in Refs. 42, 43, and 44, to synthesize a highly crosslinked 3-D network compound, which reportedly displays a BET surface area in the range of 300-1300 m^2g^{-1} and is thus naturally porous. A flame-dried three neck flask fitted with a condenser and a magnetic stirring bar was charged with melamine (313 mg, 2.485 mmol), terephthalaldehyde (500 mg, 3.728) and dimethylsulfoxide (15.5 ml) solvent and subsequently heated at 180 °C for 96 hrs under argon gas atmosphere. Upon cooling to room temperature, the precipitate was filtered and washed with an excess of anhydrous acetone, anhydrous tetrahydrofuran, and anhydrous dichloromethane. The solvents were removed under a reduced pressure by using a rotary evaporator. Final drying was done at 190 ^{o}C under vacuum in a tube furnace to produce a pale yellow powder with a yield of 64 %. Elemental analysis: for $C_{33}H_{21}N_{18}$, calculated: C, 59.19; H, 3.16.; N, 37.65 %; found: C, 45.77; H, 4.40; N, 43.19 %.

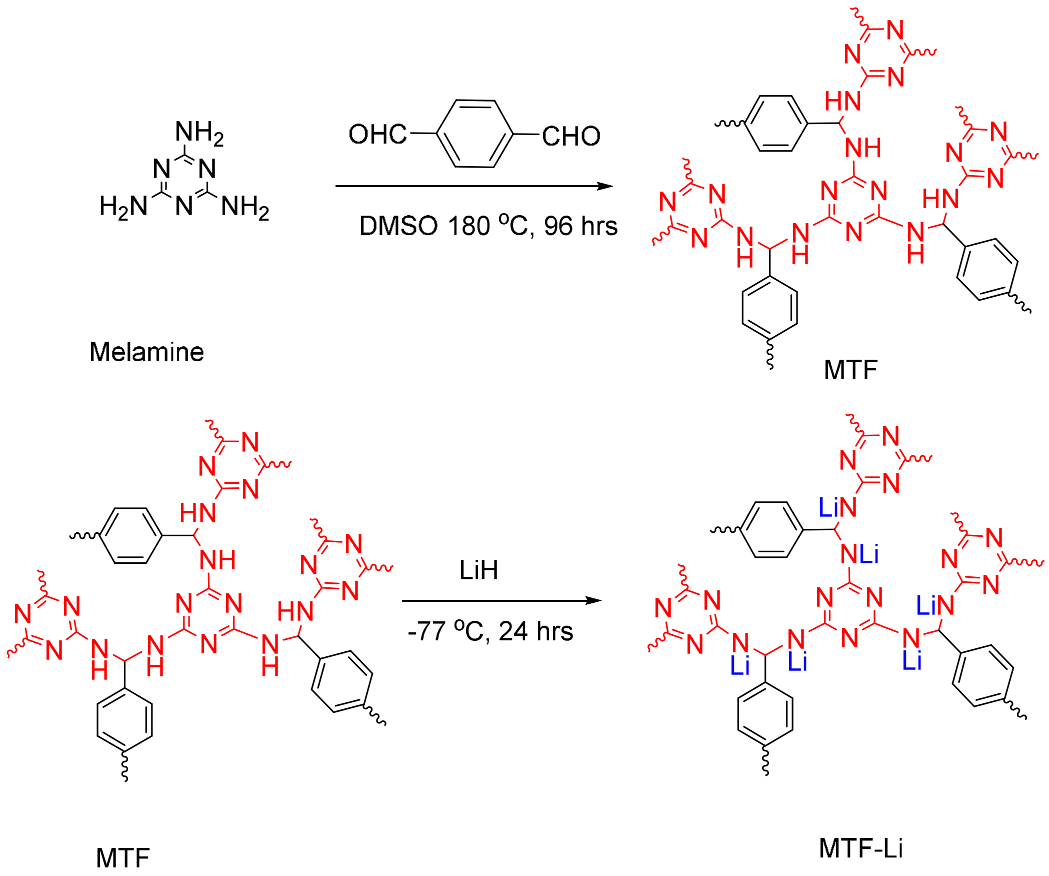

Scheme 1 Synthesis of MTF-Li complex.

In the second step, 0.5 gram of the dried framework, 0.054 gram of lithium hydride and 100 ml of dry THF were transferred to a magnetic stir fitted round bottom flask and closed with a rubber stop cock. The process was performed inside a glove box. The mixture was stirred for 24 hrs at -77 ^{o}C in a dry ice bath. The mixture was cooled to room temperature and the synthesized MTF-

Li complex was filtered and washed with an excess of anhydrous acetone, anhydrous tetrahydrofuran (THF), and anhydrous dichloromethane, respectively. The solvents were removed under a reduced pressure by using a rotary evaporator. Final drying was done at 160 ^{o}C under vacuum in a tube furnace to produce a yellow powder with a yield of 90 %. Elemental analysis: for $C_{33}H_{15}N_{18}Li_6$, calculated: C, 56.20; H, 2.14.; N, 35.75; Li, 5.90 %; found: C, 39.95; H, 4.04; N, 35.05; Li, 3.04 %.

2.2 MTF-Li/PVDF-HFP membrane preparation

MTF- Li and PVDF-HFP were mixed in different ratios, i.e., 1:1, 2:1, 1:2, in 6 ml of DMF solvent at 60 ^{o}C for 12 hrs in a 25 ml glass beaker fitted with a magnetic stirrer. The PVDF-HFP portion was dissolved easily but MTF-Li remained only in a dispersed form. Subsequently, the mixture was drop-cast into a teflon petri dish (6 cm diameter) and dried in an oven at 100 ^{o}C to vaporize the DMF solvent. The obtained film was further dried under vacuum at 100 ^{o}C for 24 hours to remove a trace amount of DMF, and then transferred to a glove box where it was punched to obtain a circular membrane with a diameter of 1.5 cm. The membrane was subsequently placed in an EC/PC (1:1 volume ratio) solution for soaking prior to use for further characterizations and performance testing in a battery cell.

3. Methods

The FTIR characterization was performed on a Bio-Rad Excalibur FTIR Spectrometer in the frequency range of 400-4000 cm^{-1}.The scanning electron microscopy (SEM) technique was used for microstructural analysis of the materials using JEOL JSM-5200 Scanning Electron Microscope. Prior to SEM analysis, the samples were sputtered with platinum under 5×10^{-2} mbar at room temperature (20s, 30mA) with a Baltec SCD050 apparatus. Thermal gravimetric analysis

(TGA) was performed under the inert atmosphere of N_2 (flow rate: 60 cm^3min^{-1}) at 10 ^oC min^{-1} heating rate, from room temperature to 1000 ^oC, in the Thermo Gravimetric Analyzer (model TGA Q 50) of TA, Inst., USA. Adsorption isotherms of N_2 were measured using a Micromeritics ASAP 2020 instrument. For the measurement, a 300 mg sample was transferred into a pre-weighted tube under inert atmosphere to prevent exposure of the sample to moisture. The sample was activated under dynamic vacuum at 100 ^oC. The warm and cold free space corrections were performed for the sample using ultra-high-purity helium gas (purity 99.9995%). The isotherms were measured in a liquid nitrogen Dewar bath at the maximum pressure range of 1 atm. An oil free pump connected with a turbo-molecular pump was used to prevent oil contamination during vacuum and feed gas in the activation process and in the isotherm measurements, respectively. The Brunauer-Emmett-Teller (BET) surface area was calculated over the range of relative pressure of 0.2 -1.0 bar.

Electrochemical impedance spectroscopy (EIS) technique was used to measure ionic conductivity of the electrolyte using the Zahner potentiostate-galvanostatate electrochemical workstation. The testing was performed in a frequency range of 4×10^6 to 1 Hz with oscillating voltage of 5 mV. A stainless steel cylindrical device of 1.5 cm diameter was used for conductivity measurement. Electrolyte membrane was placed in a stainless steel cylindrical device of 1.5 cm diameter, inside a glove box under argon atmosphere. Prior to analysis, the membrane fitted device was heated at 80 ^oC to maximize the contact between the surfaces of the device plates serving as the electrodes and the membrane. The fitting of the raw data was performed by using the Simulated Impedance Measurement (SIM) software.

A multichannel battery testing instrument Arbin BT-2000 was used for the charge and discharge capacity measurement of the coin cells assembled with the electrolyte membrane. Li metal foil and $LiFePO_4$ composite were used as an anode and a cathode, respectively, for the coin cell. The cathode was prepared by casting a well stirred solution of $LiFePO_4$ (75%), PVDF (10%), acetylene black (10%) and a small amount of lithium bis(4-carboxy phenyl sulfonyl)imide (5%), which worked as a supporting electrolyte, in NMP solvent onto an aluminum foil. The resulting electrode was dried in a vacuum oven at 80 ^{o}C for 12 hours. The dried cathode was then cut into a circular shape used in coin cells. The assembling of the standard coin cells (CR2025) was done inside a glove box.

4. Results and Discussions

4.1 Synthesis and characterization

The melamine-terephthalaldehyde complex (MTF) was synthesized with the procedure described previously.[42-46] Although the elemental analysis results differ considerably from the expected theoretical values due to the rapid crosslinking reaction, they are consistent with the reported values in the source papers. The lithium modified complex (MTF-Li), where Li atoms substitute the acidic hydrogen atoms, shows coherence with the elemental analysis of the MTF complex, confirming successful lithium modification. The found value of lithium is significantly inferior to the expected, indicating that the H atoms bonded to the N atoms in the MTF complex could not be fully reacted with LiH.

Successful synthesis of the three-dimensional network compounds MTF and MTF-Li was confirmed by FTIR spectroscopy. Figure 1 displays the FTIR spectra of melamine, terephthalaldehyde, MTF and MTF-Li. The absorption bands at 3470 and 3420 cm^{-1} (NH_2 stretching) as well as at 1650 cm^{-1} (NH_2 deformation) correspond to the primary amine groups of melamine, and the peaks at 2870 (C-H stretching of CHO) and 1690 cm^{-1} (C=O stretching) of terephthalaldehyde are absent in the MTF and MTF-Li spectra. The presence of the bands corresponding to quadrant (1554 cm^{-1} in MTF and 1560 cm^{-1} in MTF-Li) and semicircle stretching (1478 cm^{-1} in both MTF and MTF-Li) of the triazine rings confirms successful incorporation of melamine into the three-dimensional network. In addition, no vibrational signals corresponding to any imine linkage (C=N) were found in the proximity of 1600 cm^{-1} in both MTF and MTF-Li.[42, 44] The broad peak around 3400 cm^{-1} corresponds to the absorbed moisture in both MTF and MTF-Li.

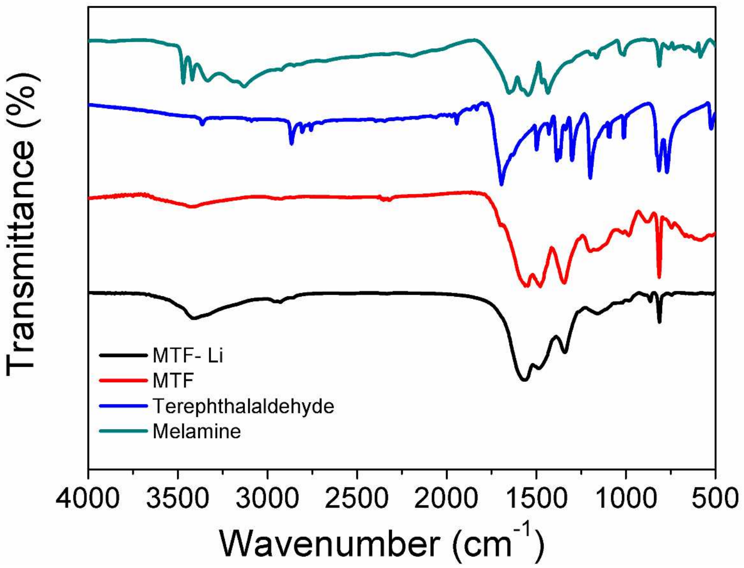

Figure 1. The FTIR spectra of melamine, terephthalaldehyde, MTF and MTF-Li complex.

The TGA thermogram of the synthesized MTF-Li is shown in Fig. 2. The MTF-Li shows a sharp weight loss after 400 °C, which is substantially higher than the degradation temperature of terephthalaldehyde (160 °C) and melamine (340 °C).[45] The higher thermal stability of the MTF-Li further confirms the success of the poly-condensation reaction and the subsequent lithiation. The MTF-Li shows an initial 10 % weight loss before 300 °C, which is attributed to the absorbed moisture or the solvents trapped in the pores of the MTF-Li complex. The major weight loss at 400 °C is due to the degradation of the triazine rings in MTF-Li.

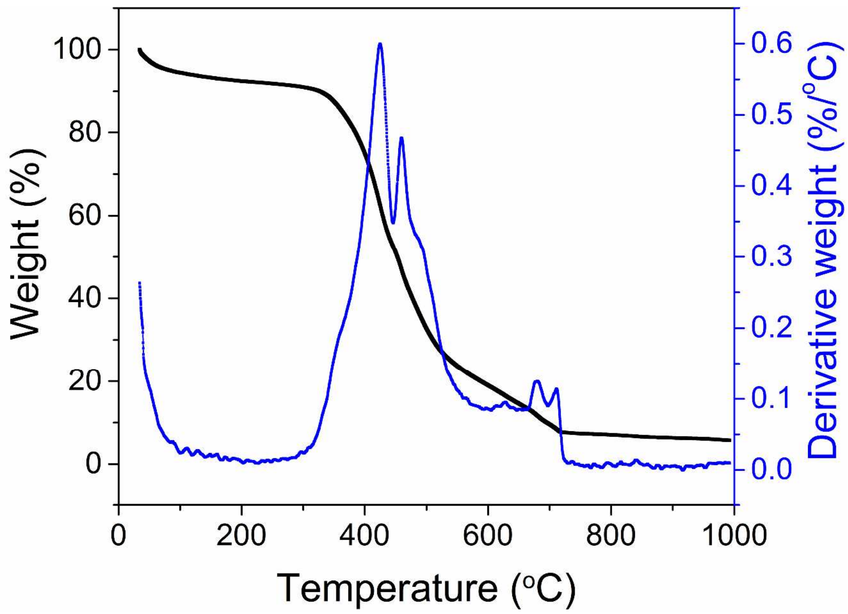

Figure 2. The TGA thermogram MTF-Li complex (N_2, 10 °C min^{-1}, RT to 1000 °C).

The specific surface area and pore size distribution (PSD) of the MTF and MTF-Li complexes were measured by nitrogen adsorption-desorption isotherms at 77K and 1 bar (Fig. 3). Both MTF and MTF-Li adsorption isotherms show a modest gas uptake at relatively low pressures and increase slowly in the middle region (Fig. 3a). This behavior confirms the meso porous nature of the synthesized MTF and MTF-Li materials.[44] The Brunauer-Emmet-Teller (BET) surface area and the Langmuir surface area of MTF were found to be 254 and 398 m^{2}g^{-1}, respectively. Upon lithiation to form MTF-Li, the measured BET and Langmuir surface areas are only reduced modestly to become 232 and 373 m^{2}g^{-1}, respectively. The DFT pore size distribution curve shows a wide range of nano-pores for both MTF and MTF-Li (Fig. 3b). In MTF, the majority of the nano-pores are in the 20-40 nm range, while in MTF-Li, the size of the nano–pores is reduced to the range of 15-20 nm, reflecting the slightly larger size of lithium as compared to hydrogen. In addition, nano-pores of 1.5- 2 nm was also detected for the MTA-Li complex, which arise mainly from inefficient packing of the molecules with a lack of topological self-complementarity.[47, 48]

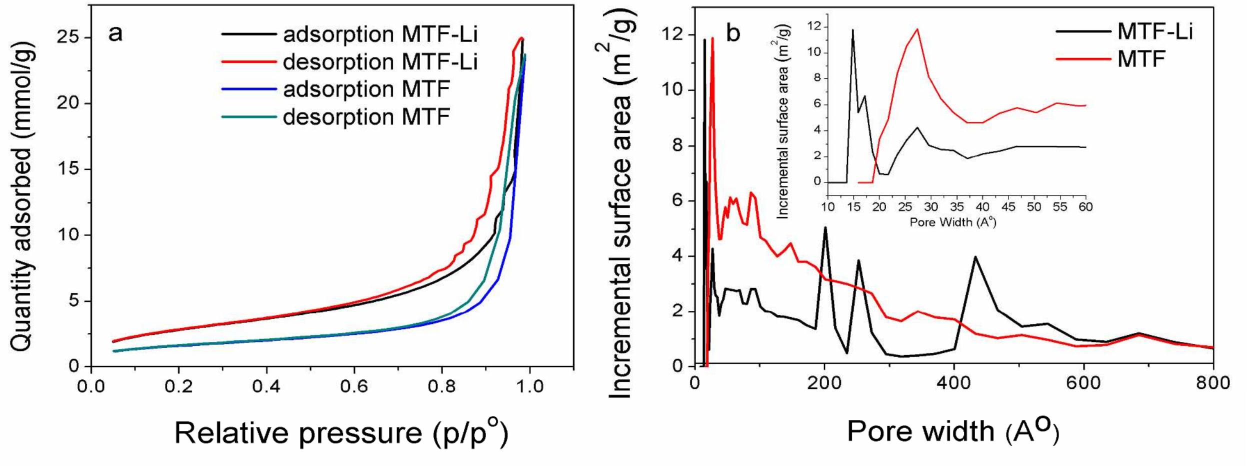

Figure 3. (a) Nitrogen adsorption-desorption isotherms at 77K and 1 bar, and (b) pore size distribution calculated from the nitrogen adsorption-desorption isotherms at 77K by applying the DFT pore size analysis method .

The porous structure of MTF-Li was further investigated by scanning electron microscopy (SEM). The SEM image of MTF-Li (Fig. 4a) reveals that a series of agglomerates are interconnected to each other to form a continuous meso-porous network. These loosely packed amorphous structures are useful to facilitate transport of Li^+ ions along with solvent molecules in electrolyte membranes.

Since the MTF-Li complex cannot be used to form a free standing membrane by itself due to its rigid three dimensional structure, it was blended with PVDF-HFP in various ratios to form single ion conducting electrolyte membranes. The membrane formed with 2:1 ratio of PVDF-HFP and MTF-Li was found most appropriate with a reasonable mechanical strength and flexibility for battery fabrication. Subsequently, the membrane was used for characterizations and battery performance testing.

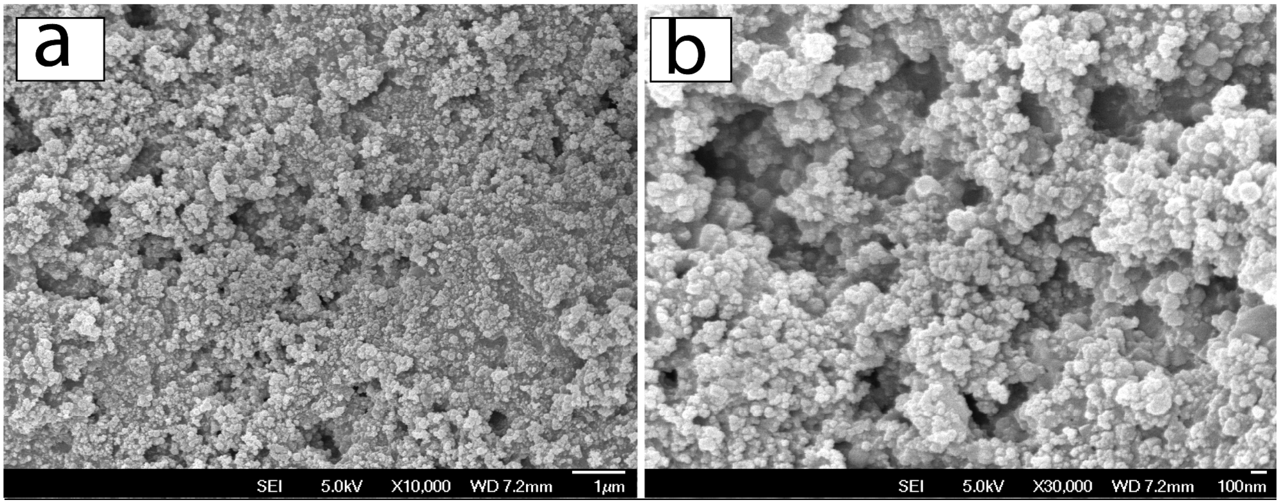

Figure 4. SEM images: a) MTF-Li, b) PVDF-HFP/MTF-Li membrane.

The SEM image of the PVDF-HFP/MTF-Li membrane is shown in Fig. 4b. The dispersed MTF-Li complex retains its porous structure in the PVDF-HFP matrix. Unlike other SIPE membranes, in which both a polymer electrolyte and a polymeric binder are dissolved in a solvent to produce a smooth and homogenous membrane upon solution casting, it is difficult to fabricate a smooth and homogenous membrane with the MTF-Li complex due to the poor solubility of MTF-Li in common organic solvents. As a result, tiny particles of MTF-Li are readily visible on surfaces of the membrane (Fig. 5). The poor uniformity of the membrane is expected to give rise to inferior interfacial resistance and thus negatively affect the battery performance. The mechanical robustness of the membrane was estimated by measuring tensile strength of the membrane. The tensile strength was found to be 3.75 MPa with 31 % elongation at break (Fig. 6), which is sufficiently high for a membrane to serve in a battery.

Figure 5. The PVDF-HFP/MTF-Li electrolyte membrane.

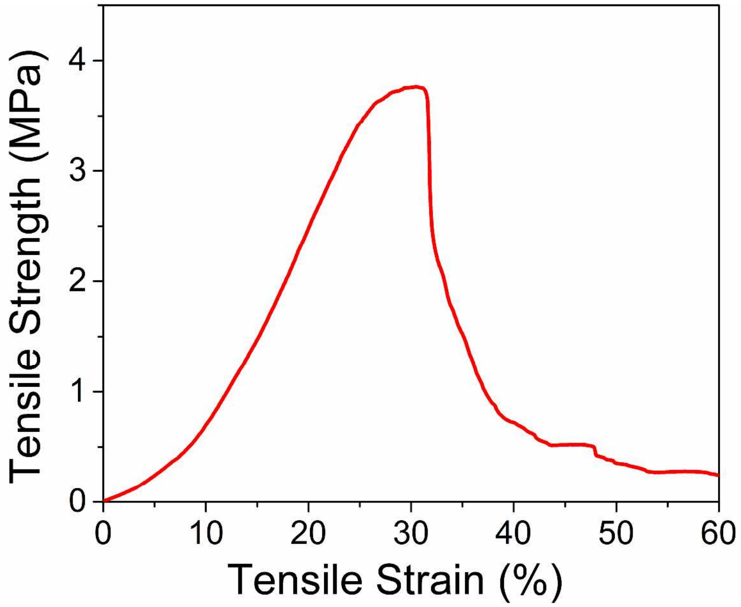

Figure 6. The tensile stress vs. tensile strain plot of PVDF-HFP/MTF-Li electrolyte membrane.

4.2 Electrochemical Properties

For EIS measurement, the PVDF-HFP/MTF-Li membrane was cut into a circular shape. The ionic conductivity of the membrane was calculated using the following equation

$$\sigma = \frac{l}{Ra}$$

where σ is the conductivity of the membrane, and *l*, *R* and *a* represent the thickness, the bulk resistance and the area of the membrane, respectively. The EIS response of the PVDF-HFP/MTF-Li (soaked in an EC/PC solution) at various temperatures in the Nyquist plots is shown in Fig. 7, where the equivalent circuit used for the fitting is also depicted. Here, R1, R2, CPE and W stand for the bulk resistance, the interface resistance, the constant phase element and the Warburg resistance, respectively. The weight of membrane was increased by 90% upon soaking in an EC/PC solution for 24 hrs.

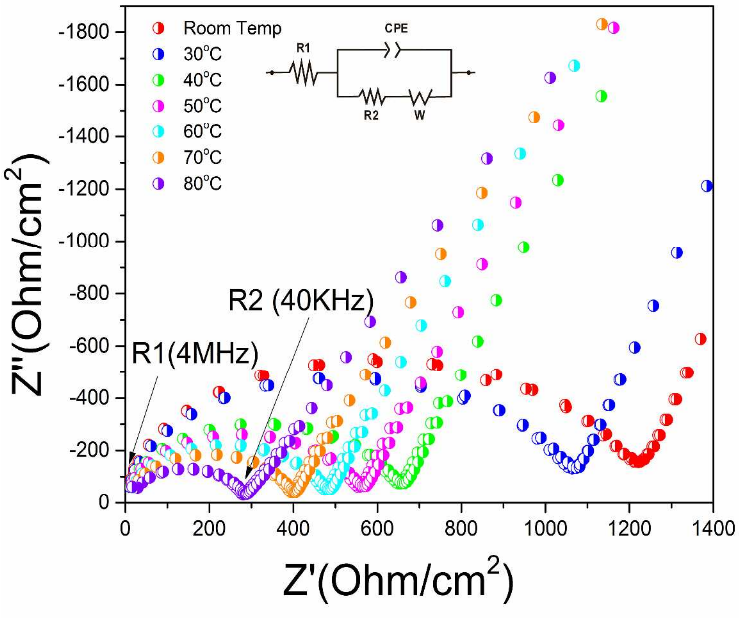

Figure 7. The EIS plot of the PVDF-HFP/MTF-Li membrane at various temperatures. The inset is the corresponding equivalent circuit.

The ionic conductivity of the membrane, based on the EIS test, was calculated to be 6×10^{-4} Scm^{-1} at room temperature, which falls into the range of conductivity displayed by most single ion gel polymeric electrolytes reported to date.[13, 49-52] The high ionic conductivity of the membrane is attributed to the weak ion pairing in the MTF-Li complex. The aromatic triazine ring allows the anionic charge to be readily delocalized, making the electrostatic interaction with Li ion relatively weak and thus promoting the cationic mobility. The high porosity of the MTF-Li complex provides smooth channels for Li ion transport mediated by the EC/PC solvent.

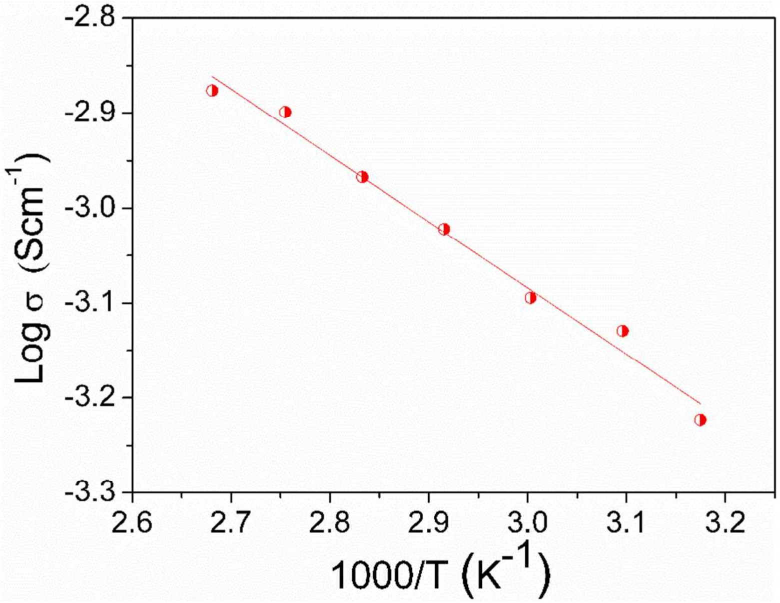

Figure 8. The Arrhenius plot of log (ionic conductivity) versus inverse of absolute temperature.

The temperature-dependency of the ionic conductivity of the PVDF-HFP/MTF-Li membrane was further investigated. Figure 8 depicts the log value of the ionic conductivity of the membrane vs. the inverse of absolute temperature, which displays coherence with a typical Arrhenius curve in the testing temperature range from 80 °C to room temperature downwards. As expected, the measured log value of conductivity increases linearly with the inverse of temperature but not as sharp as observed in small molecular electrolytes or dual-ion based gel polymer electrolytes.[53, 54] The modest rise may be attributed to the mechanical coupling between ion transport and polymer host mobility at a given temperature according to the free volume law.[55] The highest measured conductivity at 80 °C for the membrane is 1.3 ×10^{-3} Scm^{-1}. We note here that dispersing inorganic ceramic fillers in the polymer matrix may exert a positive influence on the ionic conductivity as has been demonstrated for other electrolyte materials.[56-58]

The lithium-ion transference number (t_{Li}^{+}) was measured using the Li│PVDF-HFP/MTF-Li membrane│Li assembly, where the PVDF-HFP/MTF-Li membrane swollen in an EC/PC solution beforehand was sandwiched between two non-blocking lithium metal electrodes.[10, 59] The t_{Li}^{+} measurement method, proposed by Evans and co-workers,[60] is a combination of complex impedance and potentiostatic polarization characterization techniques and was then calculated using the following equation:

$$t_{Li^{+}} = \frac{I_s\left(\Delta V - I_o R_o\right)}{I_o(\Delta V - I_s R_s)}$$

where ΔV is the DC potential applied across the cell; I_s and I_o are the steady-state and the initial current determined by the DC polarization, respectively. R_o and R_s are the EIS measured bulk resistances before and after the DC polarization (Table 1). The t_{Li}^{+} value was calculated to be 0.88 at room temperature, suggesting that the MTF-Li exhibits the typical single-ion conducting behavior as expected.

The ion transference number can also be calculated by a Li-NMR method, which might be more accurate than the method used in the present work.[61-63] The method requires knowledge of the viscosity and concentration values of the electrolyte for the calculation of transference number. Unfortunately, MTF-Li is a three dimensional network compound, which cannot be dissolved in the chosen solvent. As a result, the viscosity and concentration cannot be determined.

Table 1. Parameters for calculation of lithium ion transference number (t_{Li^+}).

ΔV	I_0 (μA)	I_s (μA)	R_0 (Ω)	R_s (Ω)	$t_{+}=\frac{I_s(\Delta V - I_0 R_0)}{I_0(\Delta V - I_s R_s)}$
0.01	1.00	0.89	5.22	7.24	0.88

The electrochemical stability of the PVDF-HFP/MTF-Li membrane was analyzed by cyclic voltammetry using the Li│PVDF-HFP/MTF-Li membrane│stainless-steel cell. The measurements, as shown in Fig 9, were performed at 25 °C between 0 and 6V (versus Li^+/Li) at a scan rate of 1 mVs^{-1}. The electrolyte membrane exhibits electrochemical stability at least above 4.0 V at room temperature, confirming its compatibility with the commercially available cathode materials.

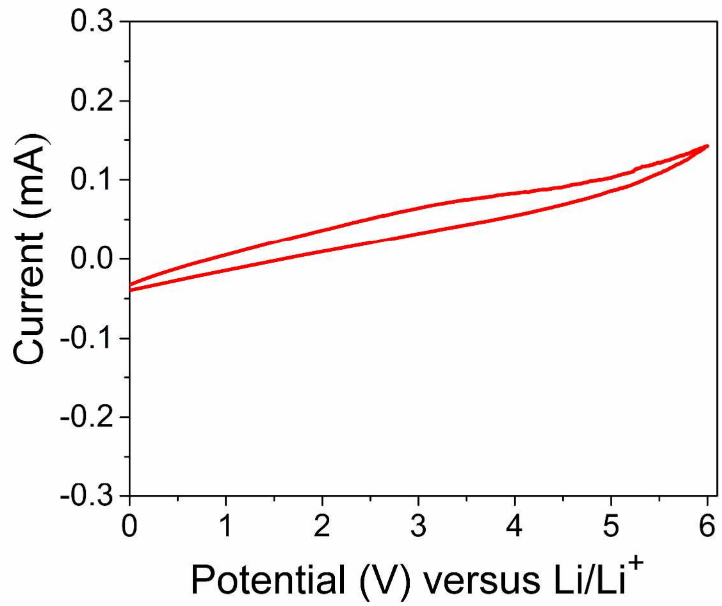

Figure 9. **Cyclic voltammetry of MTF-Li/PVDF-HFP membrane at room temperature with the scan rate of 1mVsec^{-1}.**

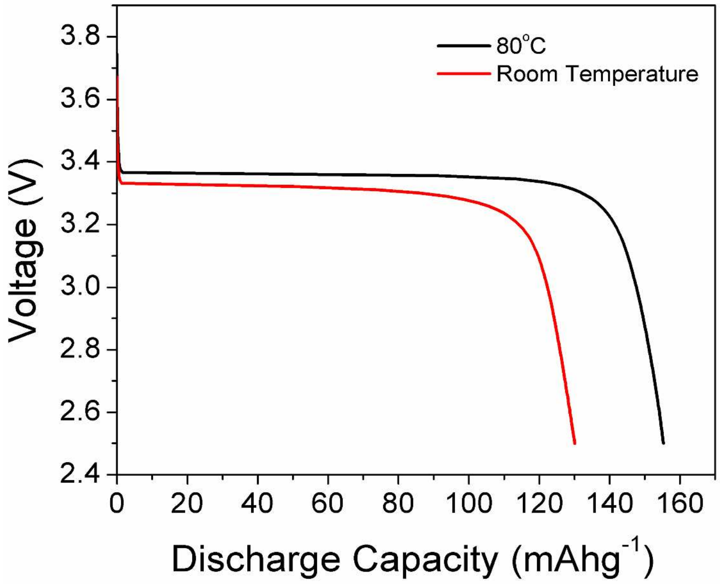

Figure 10. **The discharge profiles of the Li│PVDF-HFP/MTF-Li membrane (EC/PC)│ $LiFePO_4$ battery coin cell at room temperature and 80 °C for C/10 rate.**

To demonstrate the battery performance of the PVDF-HFP/MTF-Li membrane, we assembled a coin cell using $LiFePO_4$ as the cathode and a lithium foil as the anode. Figure 10 displays a characteristic evolution of the battery voltage of the cell Li│PVDF-HFP/MTF-Li membrane (EC/PC)│ $LiFePO_4$ as a function of its discharge capacity, at room temperature and 80 °C. The discharge curves exhibit the typical three step plateau profile of the $LiFePO_4$ cathode material with an initial discharge capacity of 130 and 155 $mAhg^{-1}$ at room temperature and 80 °C, respectively, for C/10 rate.[7, 13, 14] The discharge capacity vs. cycle number of the cell is shown in Fig. 11. At room temperature, the discharge capacity increases with each charge-discharge cycle at C/10; a fluctuation is observed at C/5, which can also be noticed in the performance at 80 °C .The initial coulombic efficiency was found to be 89% and 98% at room temperature and 80 °C, respectively. The unevenness of the membrane surface and the rigidity of the MTF-Li complex are mainly responsible for the fluctuation observed at the both temperatures.

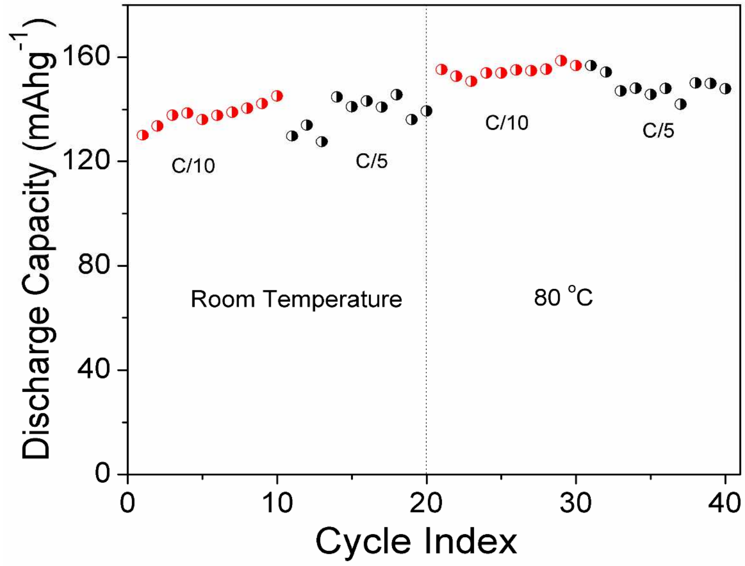

Figure 11. The discharge capacity vs. cycle index of the Li│PVDF-HFP/MTF-Li membrane (EC/PC)│ $LiFePO_4$ battery coin cell obtained at room temperature and 80 °C for C/10 and C/5 rates.

5. Summary

We present here a novel synthetic protocol for design of a melamine-terephthalaldehyde-lithium complex (MTF-Li) based single ion conducting electrolyte, where MTF-Li is a three dimensional porous network. The inherent porosity of the material allows organic solvents used in battery devices to be accommodated, leading to high Li ion mobility with the ionic conductivity on the order of 10^{-4} Scm^{-1} at room temperature, which is comparable to the value of most single ion gel polymeric electrolytes. The material shows high thermal stability and high porosity with a large surface area. It also retains its porous structure in the membrane form upon blending with a binder polymer. The electrochemical stability of the membrane was found to be sufficiently high at room temperature. While no three dimensional cross linked porous material as an electrolyte with battery performance has been reported in literature to our knowledge, the successful device operation of the MTF-Li electrolyte at room temperature reaffirms the concept that appropriate porosity of electrolyte membranes can facilitate lithium ion transport mediated by organic solvents.

Admittedly, the battery performance of the MTF-Li complex is still away from ideal for a SIPE electrolyte largely due to the low solubility of the compound in common organic solvents, which severely affects the quality of its membranes upon blending with a polymeric binder. As a consequence, surfaces of the membranes become highly uneven, leading to high interfacial resistance and ultimately inferior battery performance. Nevertheless, the present study suggests that a three dimensional porous network compound with appropriate solubility in an organic solvent can be potentially useful for synthesis of single ion conducting electrolytes. Incorporation of flexible functional groups with high electron withdrawing capability in the 3D porous network compounds could be one of the ways to develop better electrolyte materials for lithium-based battery technology.

Author Information

Corresponding Author

* chghs2@gmail.com

Author Contributions

‡These authors contributed equally.

Notes

The authors declare no competing financial interests.

Acknowledgment

The authors gratefully acknowledge support of a Start-up grant from NUS, a POC grant from National Research Foundation of Singapore, a Tier 1 grant from Singapore Ministry of Education (MOE), Singapore–Peking-Oxford Research Enterprise (SPORE), a DSTA grant and the National Natural Science Foundation of China (No. 21233006 and No. 21473164).

References

1. L. C. Hardy and D. F. Shriver, *Journal of the American Chemical Society*, 1985, 107, 3823-3828.
2. M. Doyle, T. F. Fuller and J. Newman, *Electrochimica Acta*, 1994, 39, 2073-2081.
3. B. K. Mandal, C. J. Walsh, T. Sooksimuang, S. J. Behroozi, S.-g. Kim, Y.-T. Kim, E. S. Smotkin, R. Filler and C. Castro, *Chemistry of Materials*, 1999, 12, 6-8.
4. P. G. Bruce, S. A. Freunberger, L. J. Hardwick and J.-M. Tarascon, *Nat Mater*, 2012, 11, 19-29.
5. P. G. Bruce, B. Scrosati and J.-M. Tarascon, *Angewandte Chemie International Edition*, 2008, 47, 2930-2946.
6. P. G. Bruce and C. A. Vincent, *Journal of the Chemical Society, Faraday Transactions*, 1993, 89, 3187-3203.

7. R. Bouchet, S. Maria, R. Meziane, A. Aboulaich, L. Lienafa, J.-P. Bonnet, T. N. T. Phan, D. Bertin, D. Gigmes, D. Devaux, R. Denoyel and M. Armand, *Nat Mater*, 2013, 12, 452-457.
8. K. Xu, *Chemical Reviews*, 2004, 104, 4303-4418.
9. J. N. Chazalviel, *Physical Review A*, 1990, 42, 7355-7367.
10. S. Feng, D. Shi, F. Liu, L. Zheng, J. Nie, W. Feng, X. Huang, M. Armand and Z. Zhou, *Electrochimica Acta*, 2013, 93, 254-263.
11. R. Meziane, J.-P. Bonnet, M. Courty, K. Djellab and M. Armand, *Electrochimica Acta*, 2011, 57, 14-19.
12. D. Golodnitsky, in *Encyclopedia of Electrochemical Power Sources*, eds. Juergen Garche, Chris Dyer, Patrick Moseley, Zempachi Ogumi, D. Rand and B. Scrosati, Elsevier, Amsterdam, 2009, vol. 5, ch. 112, pp. 112-128.
13. X.-G. Sun and J. B. Kerr, *Macromolecules*, 2005, 39, 362-372.
14. X. Wang, Z. Liu, C. Zhang, Q. Kong, J. Yao, P. Han, W. Jiang, H. Xu and G. Cui, *Electrochimica Acta*, 2013, 92, 132-138.
15. Y. Zhang, G. Xu, Y. Sun, B. Han, T. B. W. T, Z. Chen, R. Rohan and H. Cheng, *RSC Advances*, 2013, 3, 14934-14937.
16. W. Cai, Y. Zhang, J. Li, Y. Sun and H. Cheng, *ChemSusChem*, 2014, 7, 1063-1067.
17. R. Rohan, Y. Sun, W. Cai, Y. Zhang, K. Pareek, G. Xu and H. Cheng, *Solid State Ionics*, 2014, 268 B, 294-299.
18. Y. Sun, R. Rohan, W. Cai, X. Wan, K. Pareek, A. Lin, Z. Yunfeng and H. Cheng, *Energy Technology*, 2014, 2, 698-704.
19. G. Xu, Y. Sun, R. Rohan, Y. Zhang, W. Cai and H. Cheng, *J Mater Sci*, 2014, 49, 6111-6117.
20. G. Xu, Y. Zhang, R. Rohan, W. Cai and H. Cheng, *Electrochimica Acta*, 2014, 139, 264-269.
21. Y. Zhang, C. A. Lim, W. Cai, R. Rohan, G. Xu, Y. Sun and H. Cheng, *RSC Advances*, 2014, 4, 43857-43864.
22. Y. Zhang, R. Rohan, W. Cai, G. Xu, Y. Sun, A. Lin and H. Cheng, *ACS Applied Materials & Interfaces*, 2014, 6, 17534-17542.
23. Y. Zhang, R. Rohan, Y. Sun, W. Cai, G. Xu, A. Lin and H. Cheng, *RSC Advances*, 2014, 4, 21163.
24. Y. Zhang, Y. Sun, G. Xu, W. Cai, R. Rohan, A. Lin and H. Cheng, *Energy Technology*, 2014, 2, 643-650.
25. *Advances in Lithium- Ion Batteries*, Kluwer Academic Publishers, 2002.
26. K.-J. Lin, K. Li and J. K. Maranas, *RSC Advances*, 2013, 3, 1564-1571.
27. R. C. Agrawal and G. P. Pandey, *Journal of Physics D: Applied Physics*, 2008, 41, 223001.
28. A. Manuel Stephan, *European Polymer Journal*, 2006, 42, 21-42.
29. C. Liao, X.-G. Sun and S. Dai, *Electrochimica Acta*, 2013, 87, 889-894.
30. X.-G. Sun, J. B. Kerr, C. L. Reeder, G. Liu and Y. Han, *Macromolecules*, 2004, 37, 5133-5135.
31. X.-G. Sun, C. L. Reeder and J. B. Kerr, *Macromolecules*, 2004, 37, 2219-2227.
32. T.-H. Cho, M. Tanaka, H. Onishi, Y. Kondo, T. Nakamura, H. Yamazaki, S. Tanase and T. Sakai, *Journal of Power Sources*, 2008, 181, 155-160.
33. Y. Liang, L. Ji, B. Guo, Z. Lin, Y. Yao, Y. Li, M. Alcoutlabi, Y. Qiu and X. Zhang, *Journal of Power Sources*, 2011, 196, 436-441.
34. R. Rohan, Y. Sun, W. Cai, K. Pareek, Y. Zhang, G. Xu and H. Cheng, *Journal of Materials Chemistry A*, 2014, 2, 2960-2967.
35. C. N. Walker, C. Versek, M. Touminen and G. N. Tew, *ACS Macro Letters*, 2012, 1, 737-741.
36. Q. Shi, M. Yu, X. Zhou, Y. Yan and C. Wan, *Journal of Power Sources*, 2002, 103, 286-292.
37. M. Osińska, M. Walkowiak, A. Zalewska and T. Jesionowski, *Journal of Membrane Science*, 2009, 326, 582-588.

38. A. Banerjee, K. K. Upadhyay, D. Puthusseri, V. Aravindan, S. Madhavi and S. Ogale, *Nanoscale*, 2014, 6, 4387-4394.
39. S.-L. Li and Q. Xu, *Energy & Environmental Science*, 2013, 6, 1656-1683.
40. D. Wu, Z. Guo, X. Yin, Q. Pang, B. Tu, L. Zhang, Y.-G. Wang and Q. Li, *Advanced materials*, 2014, 26, 3258-3262.
41. B. M. Wiers, M.-L. Foo, N. P. Balsara and J. R. Long, *Journal of the American Chemical Society*, 2011, 133, 14522-14525.
42. M. G. Schwab, B. Fassbender, H. W. Spiess, A. Thomas, X. Feng and K. Müllen, *Journal of the American Chemical Society*, 2009, 131, 7216-7217.
43. L. Liu, P.-Z. Li, L. Zhu, R. Zou and Y. Zhao, *Polymer*, 2013, 54, 596-600.
44. G. Yang, H. Han, C. Du, Z. Luo and Y. Wang, *Polymer*, 2010, 51, 6193-6202.
45. K. Pareek, Q. Zhang, R. Rohan and H. Cheng, *Journal of Materials Chemistry A*, 2014, 2, 13534-13540.
46. K. Pareek, Q. Zhang, R. Rohan, G. Xu and H. Cheng, *Advanced Materials Interfaces*, 2014, DOI: 10.1002/admi.201400107, n/a-n/a.
47. J. R. Holst, A. Trewin and A. I. Cooper, *Nature chemistry*, 2010, 2, 915-920.
48. K. Pareek, Q. Zhang, R. Rohan, Z. Yunfeng and H. Cheng, *RSC Advances*, 2014, 4, 33905-33910.
49. Y. S. Zhu, X. J. Wang, Y. Y. Hou, X. W. Gao, L. L. Liu, Y. P. Wu and M. Shimizu, *Electrochimica Acta*, 2013, 87, 113-118.
50. M. Watanabe, Y. Suzuki and A. Nishimoto, *Electrochimica Acta*, 2000, 45, 1187-1192.
51. L.-Y. Tian, X.-B. Huang and X.-Z. Tang, *European Polymer Journal*, 2004, 40, 735-742.
52. X. Wang, Z. Liu, Q. Kong, W. Jiang, J. Yao, C. Zhang and G. Cui, *Solid State Ionics*, 262, 747-753.
53. J. Jiang, D. Gao, Z. Li and G. Su, *Reactive and Functional Polymers*, 2006, 66, 1141-1148.
54. A. M. Voice, J. P. Southall, V. Rogers, K. H. Matthews, G. R. Davies, J. E. McIntyre and I. M. Ward, *Polymer*, 1994, 35, 3363.
55. O. E. Geiculescu, J. Yang, S. Zhou, G. Shafer, Y. Xie, J. Albright, S. E. Creager, W. T. Pennington and D. D. DesMarteau, *Journal of The Electrochemical Society*, 2004, 151, A1363-A1368.
56. P. Raghavan, X. Zhao, J.-K. Kim, J. Manuel, G. S. Chauhan, J.-H. Ahn and C. Nah, *Electrochimica Acta*, 2008, 54, 228-234.
57. L. Hu, Z. Tang and Z. Zhang, *Journal of Power Sources*, 2007, 166, 226-232.
58. S. M. M. Yasin, S. Ibrahim and M. R. Johan, *The Scientific World Journal*, 2014, 2014, 547076.
59. A. Ghosh, C. Wang and P. Kofinas, *Journal of The Electrochemical Society*, 2010, 157, A846-A849.
60. J. Evans, C. A. Vincent and P. G. Bruce, *Polymer*, 1987, 28, 2324-2328.
61. R. Hartl, M. Fleischmann, R. Gschwind, M. Winter and H. Gores, *Energies*, 2013, 6, 4448-4464.
62. Y. Saito, H. Yamamoto, O. Nakamura, H. Kageyama, H. Ishikawa, T. Miyoshi and M. Matsuoka, *Journal of Power Sources*, 1999, 81–82, 772-776.
63. J. Zhao, L. Wang, X. He, C. Wan and C. Jiang, *Journal of The Electrochemical Society*, 2008, 155, A292-A296.

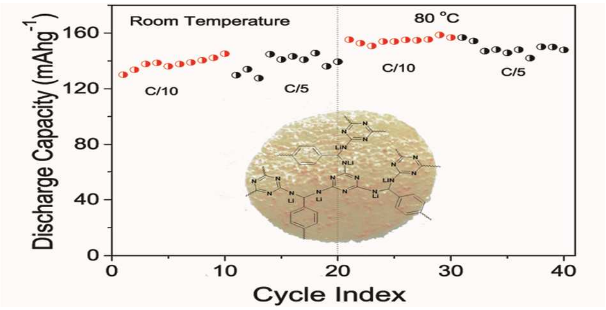

Melamine based porous organic frameworks as a single ion conducting electrolyte for lithium ion batteries.